

Application of RANSE-based Simulations for Resistance Prediction of Medium-Speed Catamarans at Different Scales

M. Haase¹, F. Iliopoulos¹, G. Davidson², S. Friezer³, G. Thomas¹, J. Binns¹, N. Bose¹, J. Lavroff⁴ and M. R. Davis⁴

¹Australian Maritime College
University of Tasmania, Launceston, Tasmania, 7250, Australia

²Revolution Design Pty Ltd
Hobart, Tasmania, 7009, Australia

³Stuart Friezer Marine Pty Ltd
Sydney, New South Wales, 2094, Australia

⁴School of Engineering
University of Tasmania, Hobart, Tasmania 7005, Australia

Abstract

Medium-speed catamarans are the latest development in fast marine transportation. Reliable methods to estimate the calm water performance and to predict the powering for the full scale vessel are necessary. For this paper RANSE-based methods were used to predict the total resistance for medium-speed catamarans for various hull forms, speeds and scales using both an open-source and commercial solver. For the Froude numbers of interest ($0.3 < Fr < 0.5$) an absolute relative error of 10% and below could be achieved compared to model and full scale test results.

Introduction

High-speed catamarans have evolved in the last two decades as an efficient vessel class for fast sea transportation. To promote sustainable sea transportation and to meet raising ecological requirements to reduce the environmental impact, a new class of large fuel-efficient medium-speed catamaran ferries is under development (Davidson et al., 2011a,b). As shown in earlier work (Haase et al., 2012a,b), medium-speed catamarans will efficiently operate at Froude numbers of $Fr = 0.35$, which is defined by $Fr = U/\sqrt{Lg}$, where U is the velocity of the vessel, L the wetted length and g the gravitational constant. Inviscid resistance prediction tools are widely used to estimate the powering requirements for ships at high and low speeds, but it has been found that they lack in the medium speed range for catamarans, which may be due to separation effects at the transom and wave-breaking between the hulls (Couser, 1997). Therefore, there is a demand for numerical tools to correctly determine the resistance of such craft independent of speed, hull form and scale.

Not only the resistance, but also the hydrodynamic phenomena occurring at this speed range between the displacement and planing regime are of interest to understand the flow for more efficient design and to predict the full scale resistance of such craft. In this paper viscous free-surface flow simulations, based on the Reynolds-averaged Navier-Stokes equation (RANSE) are utilised to investigate the calm water performance of medium-speed catamarans.

The simulations have been conducted with different solvers and hull forms, at model and full scale, to obtain an overview of the suitability of various RANSE-based methods for the performance prediction as summarised in Table 1. One solver being OpenFOAM which is open-source, the other STAR-CCM+ which is commercially available from CD-Adapco.

The advantage of full scale simulations are that the forces do not need to be scaled using an empirically determined friction line and the effects of the higher Reynolds number on the wave-making compared to model scale. The latter issue leads to a more pronounced stern wave system, as the boundary layer is thinner and a higher proportion of pressure can be recovered (Raven et al., 2008).

Presented is the first stage of a comprehensive numerical study which was to validate the computational set-up. Future work will focus on numerical self propulsion tests using waterjets, precise resistance prediction of wave-piercer catamarans (WPC) at model scale and the evaluation of design alterations of medium-speed catamarans. Previously, forces on marine vehicles have been successfully predicted by various researchers using OpenFOAM (el Moctar et al., 2010; Haase et al., 2011; Kornev et al., 2011; Maki, 2011) and CD-Adapco products (Azcueta, 2000, 2004; Azcueta and Rousselon, 2009; Bugalsky and Hoffmann, 2011).

Table 1: Summary of model set-up.

hull type	solver	Fr range	Re range
WPC	STAR-CCM+	0.32–0.49	3.2–5.0 E6
WPC	STAR-CCM+	0.17–0.60	0.4–1.4 E9
NPL	OpenFOAM	0.20–0.40	1.3–2.5 E6

Computational Set-Up

The three different simulations used different hulls and solvers, but for all the models are free to heave and trim and the free surface was modelled using the volume of fluid (VOF) approach.

Wave-Piercing Catamaran at Model Scale

This bare hull model of a wave-piercing catamaran is designed to be propeller driven and the simulations have been carried out at Froude numbers varying from 0.3 to 0.6 corresponding to Reynolds numbers of 3.2–5.0 E6. The computational domain consists of 800k cells and extends from half a ship length upstream to two and a half ship length downstream of the model in the longitudinal direction and half a ship length above and below the model. The width of the domain has been chosen so that reflecting waves do not interfere with the hull and a symmetry plane at the centre plane of the catamarans has been applied. The simulation has been conducted using STAR-CCM+ version 6, featuring dynamic fluid body interaction (DFBI) to capture heave and pitch motion, which results in a rotation and

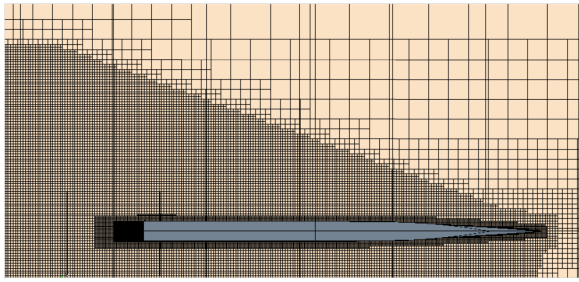


Figure 1: Structure of a hexagonal mesh for a wave-piercing catamaran created using STAR-CCM+.

translation of the entire domain. The viscous boundary layer has been modelled using a wall function and $k - \omega$ SST model with a first cell height average of $y^+ = 65$. The time step has been set to 0.01 s with 10 iterations for each step. A smaller time step has been found to not affect the results.

Wave-Piercing Catamaran at Full Scale

The model utilised for full scale simulations is different from the above as different reference data was available. The hull has been designed to be waterjet propelled and therefore the underwater geometry is different. The calm water performance has been investigated for Froude numbers of $0.17 < Fr < 0.60$ with Reynolds numbers ranging between $0.4 - 1.4 E9$. Consisting of 1,200k trimmed hexahedral cells the domain has the same dimensions compared to ship length as above, beside the clearance between hull on bottom, which equals one ship length. Refinement in the discretisation have been made close to the hull, in the wake area and for diverging waves as can be seen in Figure 1. In accordance with using a wall function, the first cell height has been chosen to not exceed a value of $y^+ \geq 100$ and the $k - \epsilon$ turbulence model has been used as by Viola et al. (2011); Bugalsky and Hoffmann (2011). As stated above the DFBI approach of STAR-CCM+ version 6 has been utilised. The time step has been chosen to be 0.1 s with a maximum of 7 internal iterations.

Fast Displacement Catamaran at Model Scale

The third model used in this study is a catamaran utilising NPL (National Physical Laboratory) hulls (Bailey, 1976; Molland et al., 1994). The Froude number ranges from 0.20–0.40 and the Reynolds number from 1.3–2.5 E6 and the domain has been discretised using 1,300k cells and stretches from one ship length upstream to four ship length downstream of the ship. The width and depth was chosen according to the towing tank in which the reference data was recorded, which is one model length downwards and one length in the transverse direction. Refinements have been done at areas with high pressure gradients and with waves diverging from the hull. Instead of a symmetry plane, the centre plane has been modelled as a solid wall without friction which showed no differences in resistance, but resulted in a more convenient dynamic mesh handling. While the mesh has also been created using STAR-CCM+, the simulations have been carried out with OpenFOAM. A multi-phase solver featuring dynamic mesh motion was utilised to resolve the free trim and heave motion of the model. The values for y^+ were chosen to be small ($y^+ \leq 11$) in conjunction with $k - \omega$ SST turbulence model due to good agreement with the ITTC ship model correlation line. For such low values and in the range of $30 < y^+ < 100$, which is recommended by Marnet-CFD, the viscous flow component of the resistance force is not very sensitive to y^+ as shown in Figure 2. The time step has been adjusted to not exceed a maximum Courant number of 2.0.

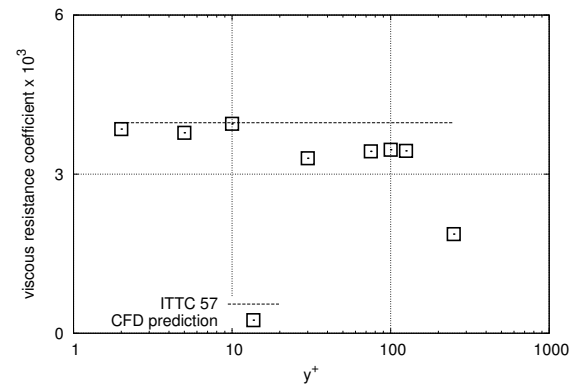


Figure 2: Force coefficient due to shear stress for different nominal values of y^+ .

Major Flow Phenomena

The forces on the hull can be simply subdivided into tangential and normal stresses, but a variety hydrodynamic phenomena occur around the demihulls of medium-speed catamarans, which need to be accurately resolved to correctly determine the overall calm water performance of such craft. So far the following have been identified:

Transom Ventilation

The transom ventilates after exceeding a certain speed. The simulations suggest a dry transom for $Fr \geq 0.30$, as can be seen in Figure 4. This agrees with findings of other researchers such as Doctors and Beck (2005). The ventilation causes ambient pressure at the separation point which leads to high pressure gradients around the edge of the transom. Compared to the pressure around the hull, a region with considerably low pressure is induced which may have a significant effect on sinkage and trim of the boat. Furthermore, behind the dry transom a significant rooster tail builds up and interacts with the wake of the opposite demihull. For lower speeds, where the transom ventilation is not present, the fluid separates at the stern and forms a confused flow at the transom, as shown in Figure 3.

Sinkage and Trim

The distribution of dynamic pressure on the hull at $Fr = 0.35$ is shown in Figure 5. At the bow there is a stagnation point resulting in high pressure (denoted as red in the figure); the pressure then reduces towards amidships (shown as light blue). Towards the stern the pressure remains low, although right at the transom it does tend to decrease rapidly. This results in a bow-up trim motion and an increase in draft, which together can cause an increase in wave resistance (Davidson et al., 2011b).

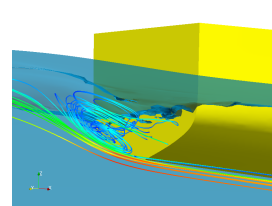


Figure 3: Flow Structure at the stern of NPL catamaran at $Fr = 0.20$.

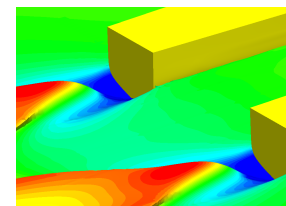


Figure 4: Dry transom and separated flow of NPL catamaran at $Fr = 0.35$.



Figure 5: Distribution of dynamic pressure on the port demihull at $Fr = 0.35$, red indicating high and blue low pressure areas.

Demihull Interaction

The demihulls are in close proximity and influence the flow around each other. This can be seen through an asymmetric pressure distribution on the wetted hull (Figure 5) as well as significant wave troughs and crests between the demihulls.

Validation

Only the simulation at model scale can be validated by comparing the predicted values of total resistance, trim and sinkage to the values measured during the model tests. For the full scale ship, no resistance test data is available, but to judge the accuracy of the resistance prediction at full scale, powering data of the vessel from sea trials have been considered as reference values. Assuming that no relevant thrust deduction occurs, it can be presumed that the resistance force is equal to the thrust produced by the waterjets. From torque measurements during sea trials and thrust diagrams for the specific waterjet unit available from the manufacturer, the resulting thrust can be estimated.

For the wave-piercer catamaran at model scale the measurements were carried out at the towing tank of AMC (Australian Maritime College) and the measurements for the NPL catamarans have been taken from the model test series of Molland et al. (1994).

Dynamic Floating Position

Both simulations at model scale show good agreements between numerically and experimentally predicted values of trim and sinkage as shown in Figure 6. Trim has been predicted within an accuracy of half a degree and the values of sinkage vary less than one percent of the draft for $Fr \leq 0.4$. For both quantities the absolute value is small and therefore the relative error may approach infinity. The simulation of the wave-piercing catamaran at $Fr = 0.49$ predicts lower absolute values than from the experiments. This may be due to a rise of the free water surface due to blockage effects or long-crested waves that may build up in the computational domain, because the accuracy of the resistance is not significantly deviating from the experimental value. Relative to the undisturbed free water surface the prediction may be more accurate. This effect has been observed with the NPL catamaran and the values presented are with respect to the undisturbed free water surface. During the sea-trials, the dynamic floating position was not measured.

Calm Water Resistance

The total resistance of the models under consideration has been made dimensionless by density (ρ), vessel length squared (L^2) and velocity squared (U^2) and plotted with respect to Froude number as shown in Figure 7. For most cases an error of around -10 % or less can be achieved as presented in Figure 8. Especially for the wave-piercing hull at model scale the error does not exceed -7 %. For the models under consideration the relative error increases for $Fr \geq 0.3$ and the resistance is underestimated, which may be due to an under-estimation of the demihull interference (Stern et al., 2006).

For the full scale simulation a higher deviation is expected due to the high uncertainty of the experimental approach. Furthermore, the computational model assumes a bare hull, while the

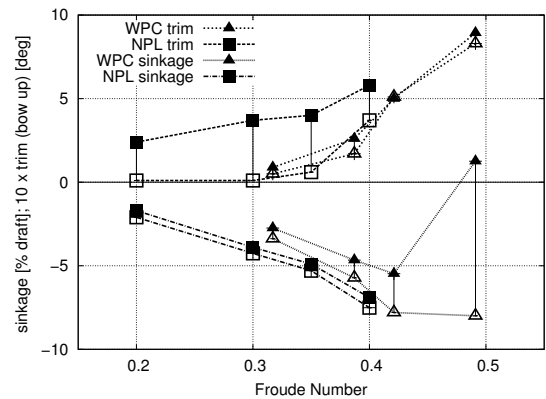


Figure 6: Trim (positive bow-up) and sinkage (negative increasing draft) of catamarans using WPC and NPL hulls at model scale from simulations (solid markers) and from experiments (hollow markers).

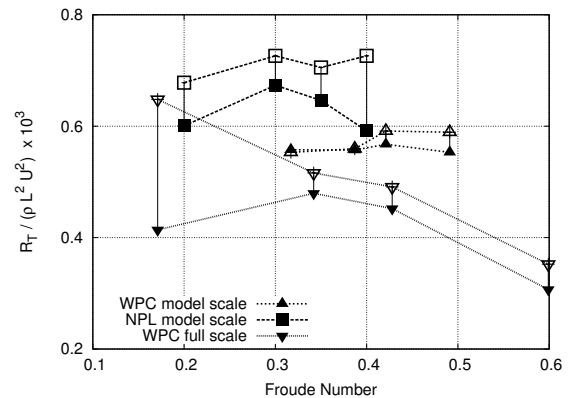


Figure 7: Total normalised resistance of three different models from simulation (full markers) and experiments or full scale trials (hollow markers).

physical model is influenced by the operating waterjets with its inlet and outlet nozzles in the stern area. At low Froude numbers where the transom is not ventilated, it is assumed that the waterjet will influence the flow past the transom significantly, which would explain the large difference between numerical and reference results. Another significant difference is that the air resistance of the ship has not been taken into account in the numerical simulation, instead an empirical force component has been added. At $Fr = 0.6$ the resistance has also been determined using $k - \omega$ SST turbulence model which leads to a smaller error (from -12.9% to -10.4%). Even though $k - \omega$ SST turbulence model is known to be unstable at large Reynolds numbers, no stability issues occurred.

For the NPL catamaran, the large error at $Fr = 0.20$ may also be due to unventilated transom, and therefore the forces developed at the transom are not accurately resolved. The deviation at $Fr = 0.40$ may be due to an under-estimate of interference and wave-breaking effects which are well pronounced in this speed range (Molland et al., 1994; Couser, 1997).

Best results have been achieved for the wave-piercer at model scale for $Fr = 0.32, 0.39$ where the absolute error is less than 1 %.

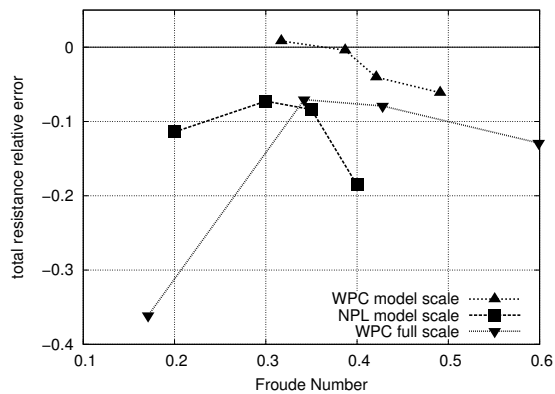


Figure 8: Relative error of total resistance prediction with respect to experimental values.

Conclusions

In this study, it has been shown that RANSE-based resistance prediction tools are capable of predicting the calm water resistance of medium-speed catamarans within a relative error of -10% independent of hull type, scale or solver used. Comparing resistance reference data derived from full scale trials to numerical predictions at the same scale is an acceptable approach to verify the numerical method, but a higher scattering as when comparing to model test results in a controlled environment has to be expected. Future work will focus on improvements in accuracy, because in further studies RANSE-based methods will be used to evaluate design alterations and to develop an approach to utilise numerical simulations to extrapolate model test data to full scale for precise powering prediction for medium-speed catamarans.

Acknowledgements

This research has been conducted as part of a collaborative research project between Incat Tasmania Pty Ltd, Revolution Design Pty Ltd, Wärtsilä Corporation, MARIN, and the Australian Maritime College at the University of Tasmania with support from the Australian Research Council's Linkage Project funding scheme, project ID: LP110100080.

*

References

- R. Azcueta. Ship Resistance Prediction by Free-Surface RANS Computations. *Ship Technology Research*, 2000.
- R. Azcueta. Steady and Unsteady RANSE Simulations for Littoral Combat Ships. In *Proceeding of 25th Symposium on Naval Hydrodynamics*, 2004.
- R. Azcueta and N. Rousselon. CFD applied to Super and Mega Yacht Design. In *Proceedings of Design Construction & Operation of Super & Mega Yachts 2009*, 2009.
- D. Bailey. *The NPL High-Speed Round Bilge Displacement Hull Series*, volume No. 4. Royal Institution of Naval Architects, 1976.
- T. Bugalsky and R. Hoffmann. Numerical Simulation of the Self-Propulsion Model Test. In *Proceeding of 2nd International Symposium on Marine Propulsors*, 2011.
- P. R. Couser. Calm Water Powering Predictions for High-Speed Catamarans. In *Proceedings of International Conference on Fast Sea Transportation*, 1997.
- G. Davidson, T. R. Roberts, S. Friezer, M. R. Davis, N. Bose, G. Thomas, J. Binns, and R. Verbeek. Maximising Efficiency and Minimising Cost in High Speed Craft. In *International Conference on Fast Sea Transportation*, volume 11, 2011a.
- G. Davidson, T. R. Roberts, S. Friezer, G. Thomas, N. Bose, M. R. Davis, and R. Verbeek. 130m Wave Piercer Catamaran: A New Energy Efficient Multihull Operating at Critical Speeds. In *Proceedings of International RINA Conference on High Speed Marine Vehicles*, pages 61–72, 2011b.
- L. J. Doctors and R. F. Beck. The separation of the flow past a transom stern. In *Proceeding of the 1st International Conference on Marine Research and Transportation*, 2005.
- B. el Moctar, J. Kaufmann, J. Ley, J. Oberhagemann, V. Shigunov, and T. Zorn. Prediction of Ship Resistance and Ship Motions Using RANSE. In *Proceeding of Gothenburg Workshop*, 2010.
- M. Haase, S. Winkler, N. Kornev, and R. Bronsart. Experimental Validation of Viscous Free Surface Flow Computation around Fast NPL Catamarans at Large Drift Angles. In *Proceedings of 1st International Symposium of Naval Architecture and Maritime*, 2011.
- M. Haase, G. Davidson, S. Friezer, J. Binns, G. Thomas, and N. Bose. On the Macro Hydrodynamic Design of Highly Efficient Medium-Speed Catamarans with Minimum Resistance. *International Journal of Maritime Engineering*, 2012a.
- M. Haase, G. Davidson, G. Thomas, J. Binns, and N. Bose. On the design and resistance prediction of large medium-speed catamarans. In *Proceeding of International Conference on High-Performance Vehicles*, 2012b.
- N. Kornev, A. Taranov, E. Shchukin, and L. Kleinsorge. Development of Hybrid URANS-LES Methods for Flow Simulations in the Ship Stern Area. *Ocean Engineering*, 38:1831–1838, 2011.
- K. Maki. Ship Resistance Simulations with OpenFOAM. In *6th OpenFOAM Workshop*, 2011.
- Marnet-CFD. Best Practice Guidelines for Marine Applications of Computational Fluid Dynamics. online.
- A. F. Molland, J. F. Wellicome, and P. R. Couser. Resistance Experiments on a Series of High Speed Displacement Catamarans Forms: Variation of Length-Displacement Ratio and Breadth-Draught Ratio. Technical Report 71, University of Southampton, March 1994.
- H. C. Raven, A. van der Ploeg, A. R. Starke, and L. Eça. Towards a CFD-based Prediction of Ship Performance - Progress in Predicting Full-Scale Resistance and Scale Effects. In *Proceedings of RINA Marine CFD Conference*, 2008.
- F. Stern, P. Carrica, M. Kandasamy, J. Gorski, J. O'Dea, M. Hughes, R. Miller, D. Hendrix, D. Kring, W. Milewski, R. Hoffmann, and C. Cary. Computational Hydrodynamic Tools for High-Speed Transports. *SNAME Transactions*, 114:55–79, 2006.
- I. Viola, R. Flay, and R. Ponzini. CFD Analysis of the Hull Resistance of Small Craft. In *Proceeding of Developments of Marine CFD*, 2011.